A Multiband Fractal Dipole Antenna for Wireless Communication Applications

Jawad K. Ali [*], Dr. Essam M. Abdul-Baki[**] & Mahir H. Hammed[**]

Received on: 10/3/2009
Accepted on:11/3/2010

Abstract

A multiband printed dipole antenna is presented for use in wireless communication applications. The proposed fractal antenna design is based on fractal geometry of the second level tent function transformation. Due to the resulting geometrical structures of a fractal tent function curve depend on the starting angles of the initial tent function, many dipole antennas have been modeled and the corresponding radiation characteristics have been evaluated. Theoretical performance of these antennas has been calculated using the method of moments (MoM) electromagnetic simulator, IE3D. Simulation results of many tent fractal dipole antennas which have been modeled show that all of these antennas have multiband resonate behavior, but this resonate behavior is different according to the starting angle for each antenna. The results have shown that these antennas have acceptable performance for VSWR$\leq$ 2 (return loss $\leq$ -10 dB), using a 50Ω feed line, at most of the resonating frequencies. This feature provides antenna designer with more degree of freedom, and makes the proposed antenna (or its monopole counterpart) suitable for use in the modern multi-functions communication systems.

Keywords: Fractal antenna, multiband antenna, printed dipole antenna, IFS (iteration function system).

هوائي ثنائي القطب متعدد النطاق الترددي للاتصالات النقالة

الخلاصة

في هذا البحث يتم استعراض هوائي متعدّد النطاق الترددي (multiband) من النوع ثنائي القطب المطبوع (printed dipole antenna) للإستعمال في تطبيقاتِ الاتصالات اللاسلكية. إنّ تصميمَ الهوائي المُقتَرَح مستند على اساس الترتيب الهندسي الجزئي(fractal geometry) لتحويل دالة الخيمة (tent function) من المستوى الثاني. وبسبب كون الاشكال الهندسية (geometrical structures) الناتجة عن منحني دالة الخيمة الجزئي تعتمد على زوايا البدء لدالة الخيمة ، تم نمذجة العديد من الهوائيات ثنائية القطب وجرى حساب مواصفات البث الخاصة بكل منها. تم حساب الأداء النظري لهذا الهوائي باستخدام الحقيبة البرمجية المتوفرةِ تجاريا IE3D . والتي تستند في اجراء التقييم باسلوب المحاكاة على طريقةِ ايجاد العزوم (MoM) . أظهرت نتائج المحاكاة للعديد من الهوائيات ثنائية القطب الجزئية التي جرت نمذجتها بان جميع هذه الهوائيات تمتلك سلوك رنينياً متعدداً غير ان هذا السلوك الرنيني يكون مختلفاً بحسب زاوية البدء الخاصة بكل هوائي. كما اظهرت النتائج بإن هذه الهوائيات تكون ذات اداء مقبول لقيمة VSWR $\leq$ 2 (return loss $\leq$ -10 dB)، باستخدام خط تغذية ذي ممانعة بقيمة 50Ω، عند غالبية ترددات الرنين. تزود هذه الميزة مصمم الهوائي بالدرجة الاكثر من الحرية في التصميم وهذا يَجْعلُ الهوائي ثنائي القطب المقترح (أو نظيره الاحادي القطب monopole) مناسبا للإستعمال في أنظمةِ الاتصال متعددةِ الوظائفَ الحديثة.

* Electrical and Electronic Engineering Department, University of Technology / Baghdad
** Engineering College, University of Al-Mustanssyriah / Baghdad

Introduction

Mandelbrot [1] defined a fractal as a rough or fragmented geometric shape that can be subdivided in parts, each of which is (at least approximately)
a reduced-size copy of the whole. Euclidean geometries are limited to points, lines, sheets, and volumes and assigns an integer number to describe the dimension of each of these geometries; where the dimension of a point is zero, and 1, 2, and 3 are the dimensions of the line, sheet and volume respectively. Fractal geometry describes objects in nature by dimensions, which are not conditionally integer numbers as the Euclidean geometry implies. Fractals can be either random or deterministic. Most fractal objects found in nature are random, that have been produced randomly from a set of non-determined steps. Fractals that have been produced as a result of an iterative algorithm, generated by successive dilations and translations of an initial set, are deterministic.

Fractals are characterized by the self-similarity, the fractional dimension and space-filling properties. The concept of a fractal is most often related with geometrical objects satisfying the criteria of self-similarity. Self-similarity means that an object is composed of sub-units and sub-sub-units on multiple levels that statistically resemble the structure of the whole object. These substructures are exactly of the shape as the original but it may be flipped, rotated, or stretched depending on the generation process producing the fractal shape.

In passive microwave circuits design, such in the design of the different types of filters, fractals have been used widely and extraordinary results were obtained. The space-filling property of fractals had led to producing miniaturized sizes of passive microwave circuits for compact wireless communication systems [2].

The use of fractals in microwave antenna design has dramatically increased in the recent years, where miniaturized and multiband antennas have to meet the challenges imposed upon the modern communication systems to be compact and multi-functional. Since the application
of the fractal concept on electrodynamics, much work has been devoted to antenna design [3-4].
The first reported small fractal antenna is the Koch dipole [3]. In this work, some of the classical features such bandwidth, resonance frequency, and radiation characteristics had been improved. Later, different fractal geometries, such as Hilbert, Peano, Minkowski, Sierpinski etc..., have been applied to dipole antenna design [5-6]. The reported designs offered astonishing results of antenna performance in the multiband behavior they possess.

In this study a fractal printed dipole antenna based on the second level (n=2) tent transformation has been presented as a candidate for use in modern multi-function communication systems. Different

antenna structures have shown to possess multiband behavior with reasonable radiation characteristics. This provides the antenna designer with more degree of freedom to satisfy the antenna radiation performance for the specified applications.

Generation of Fractal Tent Transformation

The presented fractal curve is constructed by applying geometrical transformations of a unit square with a side length *L*, representing the well-known tent function, using the transformation algorithm, which is called multiple reduction copy machine (MRCM) as proposed by [7]. This MRCM provides a good metaphor for what is known as deterministic iterated function systems (IFS) in mathematics. The MRCM generates a dynamical iterated function system (IFS), Fig. (1b).Using such an IFS, it is possible to produce a generation level in which all line segments join up to form a single path. It is clear from Fig. (1b), the IFS constructs such a curve with five transformations, and the space-filling property follows from the invariance of the initial square, the tent function, under the IFS. These five transformations, labeled as A, B, C, D, and E, which produce any fractal level from its preceding one, are summarized in Table(1).

In each transformation, more than one operation has to be performed on the original tent function, such stretching, flipping, and/or rotation. Figures (1a-d) show the details of the fractal curves generation process up to the 4th order (n = 4).

As shown in Figs.(1a-d), the constructed curve in a certain generation level (n) is simply a collage of the five transformations of the previous level (n–1). Because the initial tent function has a suitable symmetry, one can easily be misled when applying the IFS. The IFS uses the unit square with the inscribed letter **L** as an indication of the orientation as the initial square, Fig. (1a). It has been found that the total length Sn, of the tent fractal curve at the nth generation, is:

$$S_n = (\frac{7}{3})^n A_n L \qquad \ldots (1)$$

where A_n is a constant depending on the starting angle θ, of the initial tent function.

However, the value of this angle is bounded by an upper limit of θ = 63.435º; at which all the vertices of the triangle touches the square, as shown in Fig.2, and a lower limit of θ = 0º, at which the tent function is considered as a straight line of length equals to the side length, *L* of the square containing it.

The tent function, shown Fig.(2), can be described as:

$$f(x) = \begin{cases} ax, & x \le 0.5L \\ a(1-x), & x > 0.5L \end{cases} \qquad (2)$$

where a varies in the range:

$$0 \le |a| \le 2$$

for:

$$0^{\circ} \le q \le 63.435^{\circ}$$

As shown in Fig.(2), this corresponds to:

$$0 \le A \le L$$

It has also been found that A_n, in Eq. (1), is varied as [9,10]:

$$1 \leq A_n \leq 2.236$$

for the same range of the starting angle θ. It is worth to note here, that for $\theta = 63.435°$, the tent curve has no longer be a fractal after the 3rd generation step, since at the 4th generation step the resulting curve is not self-avoiding [9,10].

Nevertheless, the fractal curve can be used at this value of θ, up to the 3rd generation, since a maximum space-filling is gained according to Eq.(1), and it is still self-avoiding. Practically, if fractal curves are applied, few numbers of iterations are enough to model an antenna.

Antenna Modeling

Transformation

Since the shape of the resulting tent fractal curve depends on the initial tent function shown in Fig.(2), many fractal curves have been generated with different shapes; each corresponds to a certain starting angle θ. For convenience, these shapes are expressed in terms of the tent function height A, shown in Fig.(2). Four fractal curves corresponding to four values of A have been constructed. These values of A are L, $0.8L$, $0.6L$, and $0.4L$.

As a starting step a dipole has been modeled with a tent height equals to the side length L forming its two arms. The value of L has been adjusted such that the first resonance occurs at 2.45 GHz. This value of L has shown to be of about 0.35 λ.

The other three dipoles have been modeled using the same value of L, but with different values of A, to explore the subsequent effects of the variation of A on the multiband behavior of these antennas.

All of the modeled antennas are supposed to be fed with a coaxial cable of 50Ω characteristic impedance. The width of the dipole trace has been chosen to be 0.5% the dipole length. The multiband behavior of the modeled dipoles has been shown in Fig.(3). Total electric field radiation patterns, at the first four resonances, for each dipole have been shown in Fig.(4).

Antenna Performance Evaluation

The multiband behavior of the proposed fractal dipole antenna is shown in Fig.(3). Return loss (S_{11}) and voltage standing wave ratio (VSWR) responses corresponding to dipole antennas with $A=L$, $0.8L$, $0.6L$ and $0.4L$ have been shown in Fig.3a to Fig.3d respectively.

Results show that the 1st resonant frequency increases as A decreases. This is because the antenna length decreases with the reduction of A (and correspondingly the starting angle θ). Comparison of the conventional dipole antennas and the tent fractal dipole antennas with corresponding length, the resonant frequencies, for (VSWR≤ 2 and a 50Ω input feed), have been summarized in Table(2). The conventional half wave dipole antenna has a maximum gain of 2.148 dBi and a fractional bandwidth of (5-10)% [11,12].

The major factor which determines the bandwidth is the conductor trace width used. Thus

smaller trace widths results in a narrower bandwidth than those from larger trace widths conductors.

In Fig.(4), it is clear that at the first four resonances, all of the modeled dipoles possesses acceptable radiation patterns with reasonable values of antenna gain as compared with the conventional dipole with equal lengths.

The previously depicted results and many other important parameters for the different modeled dipole antennas, corresponding to structures with different starting angles, have been summarized in Table3. Among these parameters, most important is the antenna gain. As has been shown,
the antenna gain range between 2.16 to 7.70 dBi for the different dipoles
which is adequate for most wireless applications. Table3 demonstrates that for dipoles with larger starting angles (larger dipole lengths) wider bandwidths result in the lower gain. For lower values of the starting angle, the gain increases at the expense of the antenna bandwidth. A trade – off has to be made for certain gain-bandwidth suitable for the different applications.

Conclusions

In this paper a multiband fractal dipole antenna has been introduced. The proposed dipole antenna structure is based on second level of fractal tent transformation. Four dipole antennas with structures having different starting angles have been modeled and simulated using a method of moment (MoM) based electromagnetic simulator, IE3D from Zeland Software Inc.

Simulation results assure the flexibility in the design this antenna possesses together with reasonable radiation performance at different resonant frequencies. This antenna seems promising to be used in different multifunction communication applications. Using this antenna, many options are provided to the antenna designer to construct an antenna at the required resonant frequency with acceptable performance for the specified application.

References:

[1] B. B. Mandelbrot, "The Fractal Geometry of Nature," *W.H. Freeman and company*, New York, 1983.

[2] J. K Ali., "A New Miniaturized Fractal Bandpass Filter Based on Dual-Mode Microstrip Square Ring Resonator, " *Proceedings of the 5th International Multi-Conference on Signals, Systems and Devices, IEEE SSD'08 Conference*, Amman, Jordan, 20-23 July 2008.

[3] C. Puente, J. Romuw, R. Pous, and A. Hijazo, "Small But Long Koch Fractal Monopoe," *Electronic Letters*, vol. 38, no.1, 1998.

[4] K. J. Vinoy, K. A. Jose, V. K. Varadan, and V. V. Varadan, "Hilbert Curve Fractal Antenna: A Small Resonant Antenna for VHF/UHF Applications," *Microwave Opt. Technol. Lett*, vol. 29, no.4, pp. 215–219, May 2001.

[5] N. Cohen, "Fractal's New Era in Military Antennas, " *Journal of RF Design*, pp. 12-17, 2005.

[6] J. P. Gianvittorio and Y. Rahmat-Samii, "Fractal Antennas: A Novel Antenna Miniaturization Technique and Applications," *IEEE Antennas and Propagation Magazine*, vol. 44, no.1, pp.20-36, February 2002.

[7] H. Peitgen, H. Jürgens, D. Saupe, "Chaos and Fractals," *New Frontiers of Science, Second Edition, Springer-Verlag,* New York, 2004.

[8] M. H. Hammed, " Design and Simulation of multiband Fractal Antenna for Wireless Communication," *M.Sc. Thesis, Al-Mustansiriya University,* Baghdad, 2009.

[9] J. K. Ali, "A New Fractal Printed Dipole Antenna Based on Tent Transformations for Wireless Communication Applications," *Al-Khwarizmi Engineering Journal, University of Baghdad,* vol. 4, no.3, pp.57-64, April 2008.

[10] J. K. Ali, and A. H. Ahmed, "A New GCPW-Fed Fractal Monopole Antenna Based on Tent Transformations for Modern Communication Systems," *journal of Engineering and Applied Sciences*,vol.3, no.6, pp.462-470, 2008.

[11] C. A.Balanis, "Antenna Theory: Analysis and Design", 2nd ed., Wiley, 1997.

[12] W. L.Stutzman and G. A.Thiele, "Antenna Theory and Design", 2nd ed., John Wiley & Sons: New York, 1998.

Table (1) Summary of steps to generate a fractal tent transformation [8].

Step	Width stretched by	Height stretched by	Flipping	Rotation (deg.)
A	2/3*L*	1/3 *L*	horizontal	None
B	1/3 *L*	2/3 *L*	horizontal	None
C	1/3 *L*	2/3 *L*	horizontal	90
D	2/3 *L*	1/3 *L*	None	-90
E	2/3 *L*	2/3 *L*	None	-90

Table (2) Resulting resonant frequencies of the modeled fractal dipole antennas together with their equivalent length conventional dipole antennas.

		Resonant frequencies			
Antenna starting angle	Conventional dipole antenna f_0 (GHz.)	1st resonant f_{01} (GHz.)	2nd resonant f_{02} (GHz.)	3rd resonant f_{03} (GHz.)	4th resonant f_{04} (GHz.)
63.435°	1.2746	2.446	4.432	6.425	7.850
57.995°	1.5	3.035	5.705	7.58	9.515
50.194°	1.8	3.8	4.664	7.504	9.585
38.660°	2.1973	4.572	5.9	6.864	10.296

Table (3) Summary resulting antenna parameters corresponding to different starting angles

Antenna starting angle	Resonant frequencies (GHz.)		Antenna parameters							
			Rad. Eff. (%)	Ant.Eff. (%)	G (dBi)	D (dBi)	Beam width	BW (%)	VSWR	S_{11} (dB)
63.435°	f_{01}	2.446	95.87	95.37	2.16	2.36	63.79°	40.9	1.35	-21.15
	f_{02}	4.432	98.99	91.05	6.70	7.11	40.85°	9.74	1.87	-10.5
	f_{03}	6.425	100	99.43	4.84	4.86	31.24°	8.56	1.54	-16.5
	f_{04}	7.850	100	96.75	7.17	7.31	27.9°	8.92	1.65	-18.13
57.995°	f_{01}	3.035	99.86	99.33	2.62	2.65	65.46°	32.95	1.32	-21.5
	f_{02}	5.705	98.99	91.05	6.70	7.11	40.85°	5.26	1.7	-11.5
	f_{03}	7.58	100	99.43	4.84	4.86	31.24°	10.55	1.32	-21.5
	f_{04}	9.515	100	96.75	7.17	7.31	27.9°	15.76	1.54	-15
50.194°	f_{01}	3.8	100	93.83	3.38	3.66	40.83°	13.15	1.8	-12.1
	f_{02}	4.664	100	99.77	7.70	7.71	23.1°	21.44	1.23	-24
	f_{03}	7.504	89.23	82.53	7.50	8.33	32.7°	10.66	1.82	-11.9
	f_{04}	9.585	100	99.83	5.64	5.65	20.8°	16.7	1.1	-27.2
38.660°	f_{01}	4.572	100	96.85	4.70	4.83	28.3°	13.12	1.6	-15
	f_{02}	5.9	100	99.62	6.24	6.26	24.2°	13.56	1.28	-22.1
	f_{03}	6.864	100	97.15	4.31	4.43	43.94°	7.28	1.65	-15.2
	f_{04}	10.29	100	99.69	4.77	4.78	27.4°	12.3	1.35	-21.15

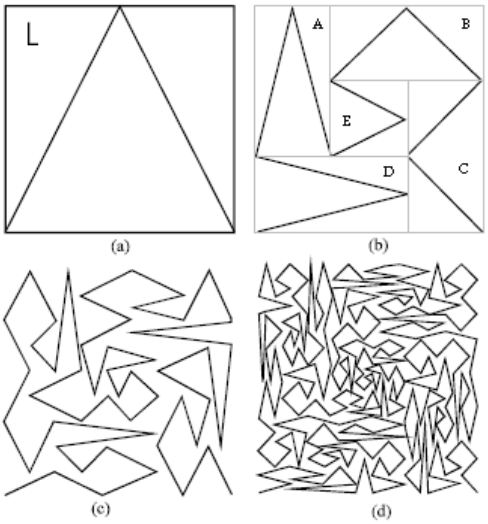

Figure (1) The details of the generation steps of the tent fractal curves. Structures from (a) to (d) correspond to the first four generation levels

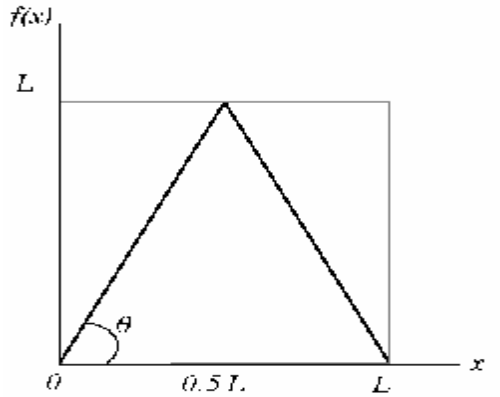

Figure (2) The tent function with side length, *L* and a starting angle, $\theta = 63.435°$

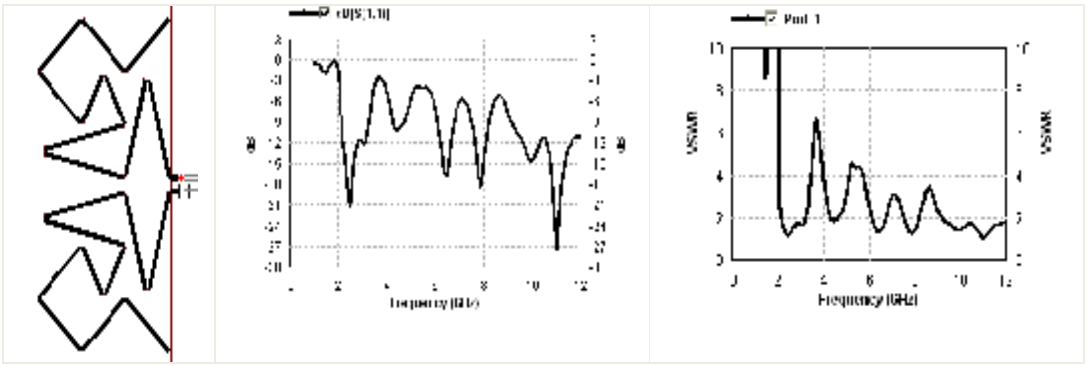

(a)

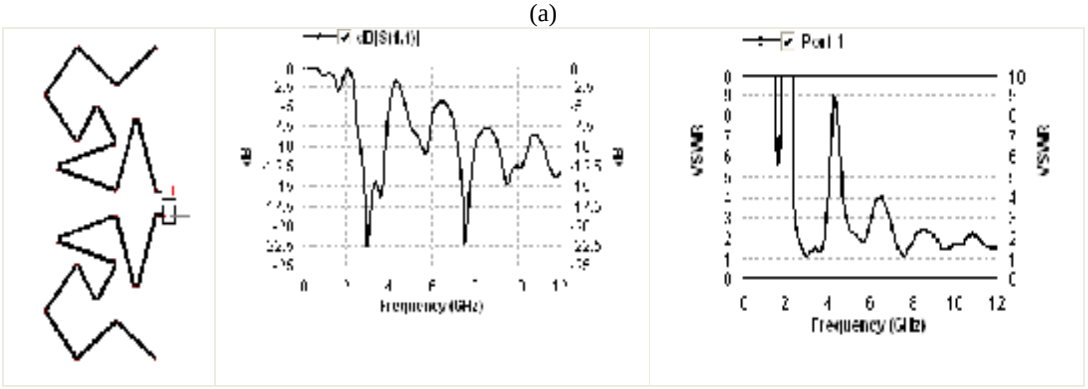

(b)

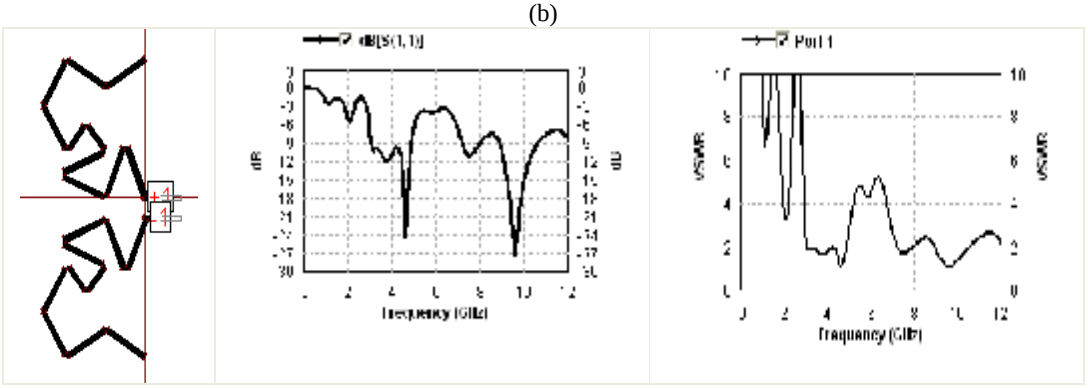

(c)

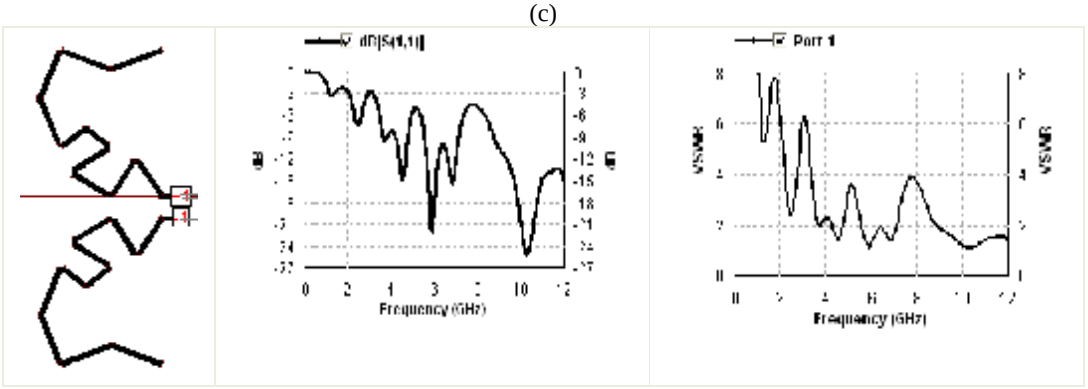

(d)

Figure (3) The modeled dipole antenna layouts and return loss and VSWR responses for fractal tent dipole antennas with (a) $A=L$, (b) $A=0.8L$, (c) $A=0.6L$, and (d) $A=0.4L$

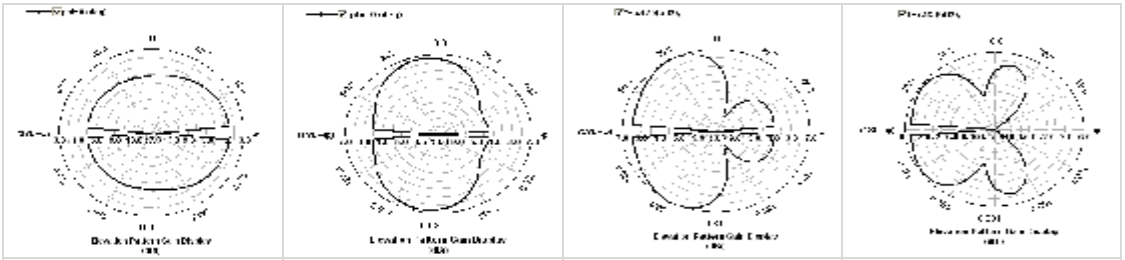

2.446 GHz.	4.432 GHz.	6.425 GHz.	7.850 GHz.

(a)

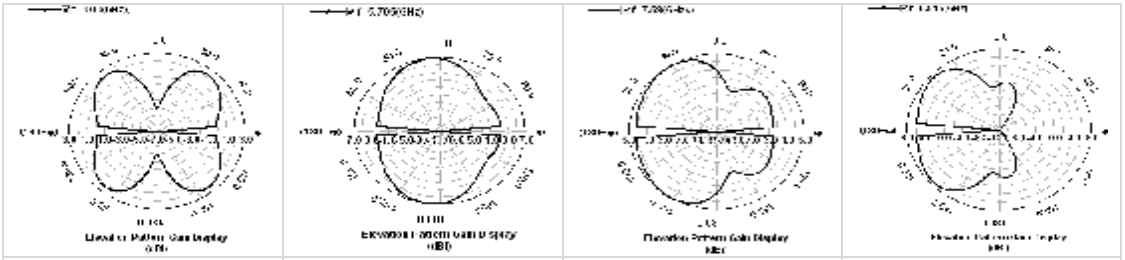

3.035 GHz.	5.705 GHz.	7.580 GHz.	9.515 GHz.

(b)

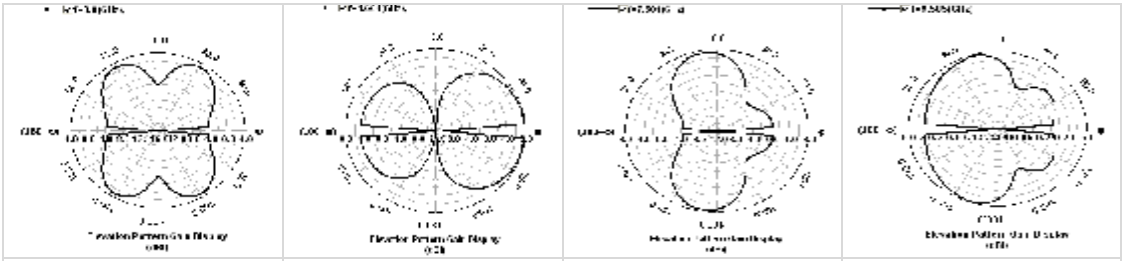

3.802 GHz.	4.664 GHz.	7.504 GHz.	9.585 GHz.

(c)

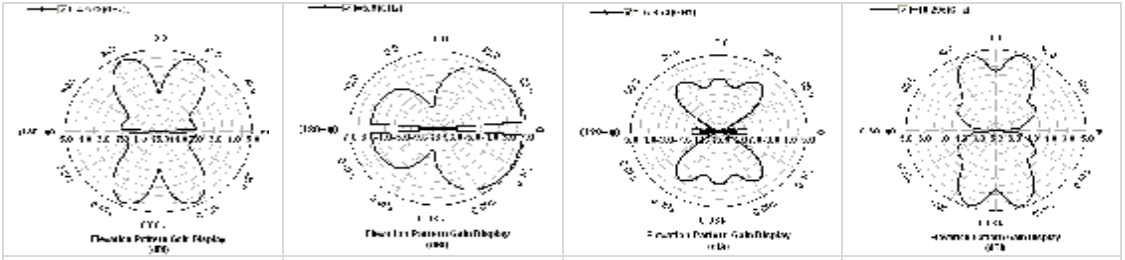

4.572 GHz.	5.901 GHz.	6.864 GHz.	10.296 GHz.

(d)

Figure (4) Elevation pattern gain display for the first four resonances for the modeled, fractal tent dipole antennas (a) $A=L$, (b) $A=0.8L$, (c) $A=0.6L$, and (d) $A=0.4L$